Journal of Materials Chemistry A

Accepted Manuscript

ROYAL SOCIETY OF CHEMISTRY

www.rsc.org/materialsA

One-Pot Facile Synthesis of Mesoporous Carbon and N-doped Carbon for CO_2 Capture by a Novel Melting-Assisted Solvent-Free Method

Zhongzheng Zhang,[†] Baodeng Wang,[†] Chenming Zhu,[†] Peng Gao,[†]
Zhiyong Tang,[†] Nannan Sun,*[,†] Wei Wei*[,†,‡] and Yuhan Sun[†,‡]

[†]CAS Key Laboratory of Low-Carbon Conversion Science and Engineering, Shanghai Advanced Research Institute, Chinese Academy of Science, Shanghai 201203, China
[‡]School of Physical Science and Technology, ShanghaiTech University, Shanghai 201210, China

Abstract: A facile and efficient one-pot melting-assisted solvent-free method is successfully developed for the first time to produce hierarchically mesoporous carbon and nitrogen-enriched mesoporous carbon materials. Such method used a very simple thermal treatment process instead of the normally reported solvent-based preparation, thus making it very potential for fast and large scale production of mesoporous carbons. The obtained carbon materials were comprehensively characterized by X-ray diffraction, Raman spectra, N_2 sorption, scanning electron microscopy, transmission electron microscopy, CHN analyzer, X-ray photoelectron spectroscopy, and elemental mapping. The results show that the as-synthesized carbon materials possess well-developed hierarchical porous structures, uniform pore sizes, and high surface areas, the specific structures can be adjusted by changing temperatures and durations of the thermal treatment process. Besides, the resultant carbon material with a high surface area of 748 m^2/g exhibits excellent CO_2 capture properties with a capacity of 2.73 mmol/g at 298 K and 1 bar, and a CO_2 selectivity of 21.6 under flue gas conditions. More importantly, due to the successful incorporation of large amounts of highly dispersed N in the carbon matrix (11.67 %), the as-synthesized NMC sample exhibits a significantly enhanced CO_2 capacity of 1.66 mmol/g with an excellent CO_2 selectivity of 240.7 at 348 K and 1 bar, revealing a great promise for practical CO_2 capture applications.

1 Introduction

CO_2 capture by adsorption using porous solid materials has attracted considerable attention due to its low cost and high-energy efficiency. Adsorbent is the core of adsorption, thus various porous materials including zeolites, activated carbons, mesoporous silica/carbon, metal oxides, and metal organic frameworks (MOFs) have been explored and investigated extensively for CO_2 capture. However, CO_2 capacity on zeolites is limited,[1,2] and has been shown to be greatly reduced in the presence of water due to the negative effect of water on the stability of the zeolite frameworks.[3] Metal oxides and MOFs exhibit high CO_2 capacities,[4,5] but the high regeneration temperature of 300-900 ^oC for metal oxides,[6,7] and the stability as well as synthesis cost of MOFs restricted their practical applications.

On the other hand, porous carbon materials, especially mesoporous carbons (MCs), have been considered as potential CO_2 adsorbents due to their ordered pore structure, high surface area, large pore volume, good adsorption capacity, low price, nontoxicity, high chemical stability

and ease of surface decoration.[8-10] Up to now, there have been many approaches for the fabrication of MCs,[11] however, a competitive method suitable for the fast, facile, and large scale synthesis of MCs is yet to be developed. For example, the commonly used nanocasting method used a sacrificial hard templates such as zeolites or mesoporous silica.[12-15] Although the obtained MCs from this method exhibit well-developed mesoporous structure and excellent textural properties, this method is time-consuming, step-tedious and costly because of the pre-preparation of the hard template, subsequent impregnation of carbon precursor and the final removal of the hard template with corrosive agents such as HF or NaOH which usually result in unwanted environmental concerns.[16-19] Compared with the nanocasting method, another widely used method is evaporation induced self-assembly (EISA), where amphiphilic surfactant or block copolymer is directly used as structure-directing agents, thus the method is much simple and facile in fabricating MCs because of the avoidance of extra steps to prepare and remove the hard template.[20-22] However, it still suffers from long preparation durations for the formation of mesostructured composite between carbon precursors and surfactant in diluted solutions though self-assembly process, which leads to low efficiency.[23,24] Furthermore, the use of large amounts of solvents inevitably causes environmental pollution and increases the fabrication cost of MCs. Therefore, both the nanocasting method and EISA method are difficult to be extended in larger scale for industrial production of MCs, and thus a simple, facile and easily industrialized strategy for MCs synthesis is highly desired.

Herein, we present a highly efficient one-pot melting-assisted solvent-free strategy to synthesize mesoporous carbons with well-ordered mesostructures, uniform pore sizes and high surface areas, which were obtained by *in situ* copolymerization of resorcinol, p-phthalaldehyde and Pluronic F127 under self-pressurized solvent-free conditions. Compared with the previously reported methods, this method only involves a simple thermal treatment procedure and avoids the use of solvents, thus exhibiting important potential for the large scale preparation of MCs in industry level. Moreover, through directly introducing nitrogen precursors in the thermal treatment process such as melamine, this method was also able to prepare nitrogen-doped porous carbons, which exhibit high nitrogen content, high surface area and excellent CO_2 adsorption capacity.

2 Experimental

2.1 Chemicals

Resorcinol, p-phthalaldehyde, and melamine were of analytical grade, purchased from Aladdin Industrial Inc. Pluronic F127 was purchased from Aldrich. All chemicals were used as received without any further purification.

2.2 Synthesis procedures

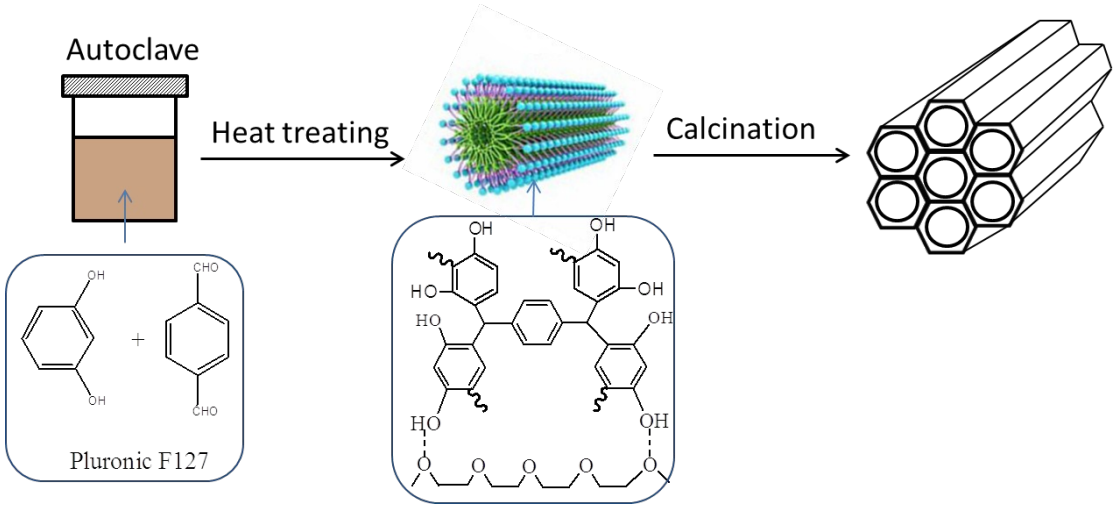

Scheme 1 Schematic illustration of the one-pot facile synthesis of MCs

Scheme 1 illustrates the schematic fabrication process of MCs with the one-pot melting-assisted solvent-free method. In a typical synthesis, solid mixture of 3.00 g of F127, 0.88 g of resorcinol, and 1.12 g of p-phthalaldehyde was sealed in an autoclave and then heated at given temperatures (100, 150, 200 and 250 ^{o}C) for given durations (such as 4, 8 and 12 h) to achieve self-assembly between carbon precursors and surfactant. The obtained dark brown material was then carbonized under nitrogen atmosphere at 800 ^{o}C for 5 h. According to the thermal treatment temperature and duration, the obtained carbon material was denoted as MC-*x*D*y*H where *x* and *y* represent the curing temperature and duration, respectively.

Nitrogen-doped mesoporous carbons can be similarly prepared by addition of melamine as a nitrogen source. For example, mixture of 3.00 g of F127, 0.88 g of resorcinol, 1.12 g of p-phthalaldehyde and 8.0 g of melamine was heated at 250 ^{o}C for 8 h in an autoclave, and then carbonized at the same conditions of MCs mentioned above. The as-synthesized nitrogen-doped carbon material was denoted as NMC-250D8H.

2.3 Characterization

The composition and phase purity of the obtained carbons were analyzed by X-ray diffractometry (XRD) on a Bruker D8 Advance instrument with Ni-filtered CuK_{α} radiation operating at 40 kV voltage and 30 mA current. The small angle XRD patterns were collected from 0.5^{o} to 5^{o}with a scanning step of 0.02^{o}, while the wide angle XRD patterns from 5^{o} to 90^{o} at a scanning step of 4^{o}. Raman spectra were recorded on a RM 2000 microscopic confocal Raman spectrometer with an excitation of 514 nm laser light at 0.5 mW and were accumulated three times for 30 s each.

Morphology of the as-synthesized samples were investigated using scanning electron microscope (SEM) on a SUPRRA^{TM} 55 apparatus with an acceleration voltage of 2.0 kV, and transmission electron microscope (TEM) was performed on a JEOL 2100F apparatus with an acceleration voltage of 200 kV. X-ray photoelectron spectroscopy (XPS) was carried out on a Quantum 2000 electron spectrometer using Al K irradiation.

The Brunauer-Emmett-Teller (BET) surface area of the obtained samples was measured using the Quantachrome Autosorb IQ_2 analyzer by N_2 sorption at 77 K. The pore size distribution (PSD) was derived from the adsorption branch of N_2 isotherms using the density functional theory (DFT) method. The total pore volume of sample was calculated from the N_2 sorption amount at the

relative pressure of 0.995, and the micropore area and volume were estimated by t-plot method.

CO_2 sorption isotherms were measured at different desired temperatures using a Micromeritics ASAP 2020 instrument. Prior to each adsorption measurement, the samples were degassed at 200 ^oC for 8 h to remove the guest molecules from pores.

3 Results and discussion

3.1 Structural characteristics of the MCs

As has been well documented, the temperature and duration of the thermal treatment process are crucial experimental parameters in determining the self-assembly and copolymerization of the surfactant with the precursors. Hence, different curing temperatures in our experiments were firstly investigated in order to study their influence on the structure and textural properties of the resultant carbon materials.

The small angel XRD patterns of the samples obtained at different curing temperatures for 8 h are exhibited in Fig.1A. It can be clearly seen that the pattern of the MC-100D8H sample obviously reveals two resolved diffraction peaks at 2θ of ca. 0.96^o and 1.65^o, which can be associated with (100) and (200) reflections of a typical 2-D hexagonal structure, respectively. This indicates the presence of mesoporous structure in the MC-100D8H sample with highly developed long range ordering. With the increase of curing temperature, the peak assigned to (200) reflection of the 2-D hexagonal structure disappears, but the intensity of the (100) peak remains strong although a little decrease was observed, indicating the samples obtained at elevated temperatures still exhibit mesostructures only a slightly lower structural ordering as compared with that of the sample MC-100D8H. Generally, the higher the curing temperature is, the broader of the diffraction peak and the lower of the peak intensity becomes. Furthermore, the peak position of MC-200D8H and MC-250D8H undergoes an obvious shifting to lower angle, which is indicative of a larger spacing probably owing to the swelling of F127 micelles in the surfactant-polymer composites at a high temperature.[25,26]

The wide angle XRD patterns presented in Fig.1B show that all the samples exhibited two obvious broad diffraction peaks at 2θ = 22.4^o and 43.5^o, which correspond to (002) and (100) diffractions of amorphous carbon, respectively.[27,28] The result reveals that the as-obtained carbons possess low crystallinity, this is well in accordance with the Raman spectra results as shown in Fig.2, where all the samples show two broad representative bands, the D band at around 1343 cm^{-1} related to defects and the G band at around 1600 cm^{-1} related to the ordered SP^2 bonded carbon. The ratio of peak intensity (I_D/I_G) for all samples is around 1.0, which is indicative of the defective structures of the obtained carbon materials.[29,30]

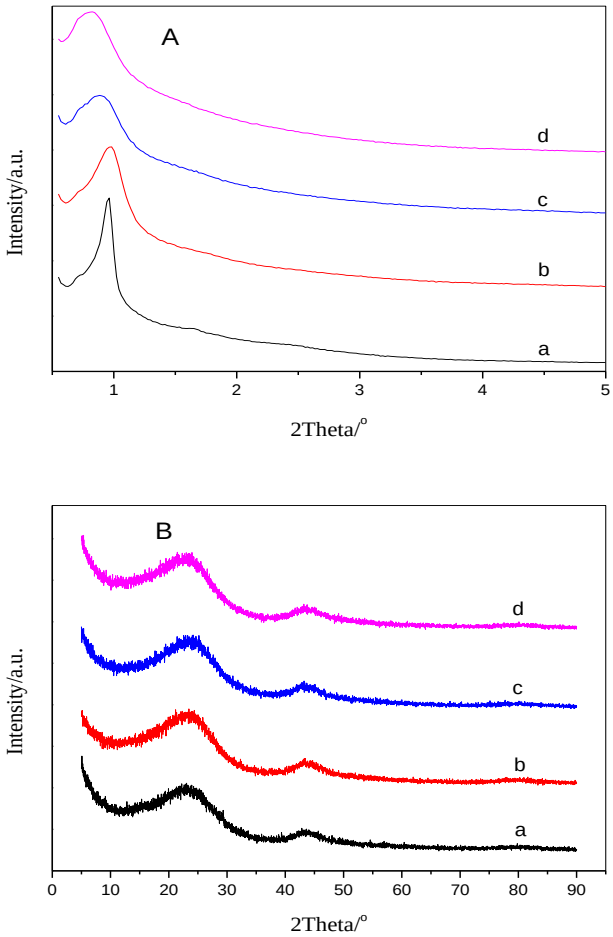

Fig.1 Small (A) and wide (B) angle XRD patterns of the samples prepared at different temperatures for 8 h. (a) MC-100D8H, (b) MC-150D8H, (c) MC-200D8H and (d) MC-250D8H

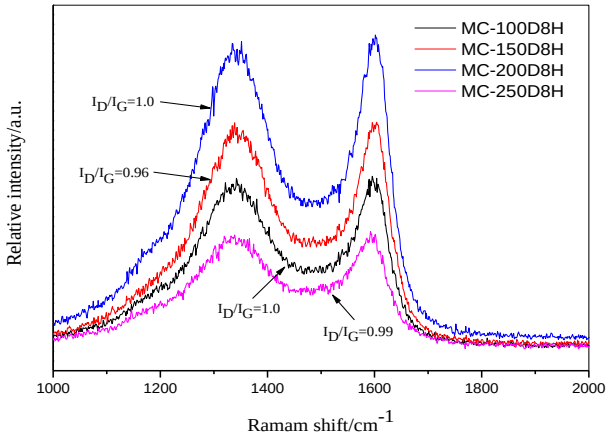

Fig.2 Raman spectra of the obtained carbons prepared at different curing temperatures

The nitrogen sorption isotherms and corresponding pore size distributions of the samples are shown in Fig.3. In Fig.3A, all isotherms are of type IV with a pronounced hysteresis loop in the relative pressures range of ca. 0.4-0.7, at the same time, a sharp N_2 uptake is observed at low relative pressure (p/p^0<0.02), indicating the presence of substantially developed micropores and

mesopores with small pore size, this can be further confirmed by the corresponding PSD curves in Fig.3B where two obvious peaks of mesopores around 2 nm and 5 nm, and a narrow micropore peak at ca. 1.0 nm are observable. The formation of the micropores is probably due to the dehydrogenation and deoxygenation from the polymeric frameworks, while the mesopores are generated by the removal of the template owing to the difference in chemical and thermal stability between the carbon precursors and template during the transformation of the polymeric frameworks to carbon mesostructures.[31,32] With the increase of thermal treatment temperature, the pore size, especially the larger mesopores, exhibits an obviously increasing trend from 4.53 to 5.15 nm, which could be attributed to the larger thermodynamic diameter of F127 micelle at higher temperatures,[33, 34] thus leaving larger mesopore size after its removal. In addition, it can be seen from Tab.1 that the pore volumes of the samples gradually increased from 0.37 to 0.60 cm^3/g as the curing temperature rose from 100 to 250 ^oC, while the specific surface area reached a maximum of 748 m^2/g at 200 ^oC and further increase of the thermal treatment temperature makes almost no changes in the surface area. Furthermore, one can see that the major contribution to the specific surface area of all samples arises from the micropores, for example, the micropore surface area of the sample MC-200D8H is as high as 509 m^2/g, accounting for 68 % of its total surface area.

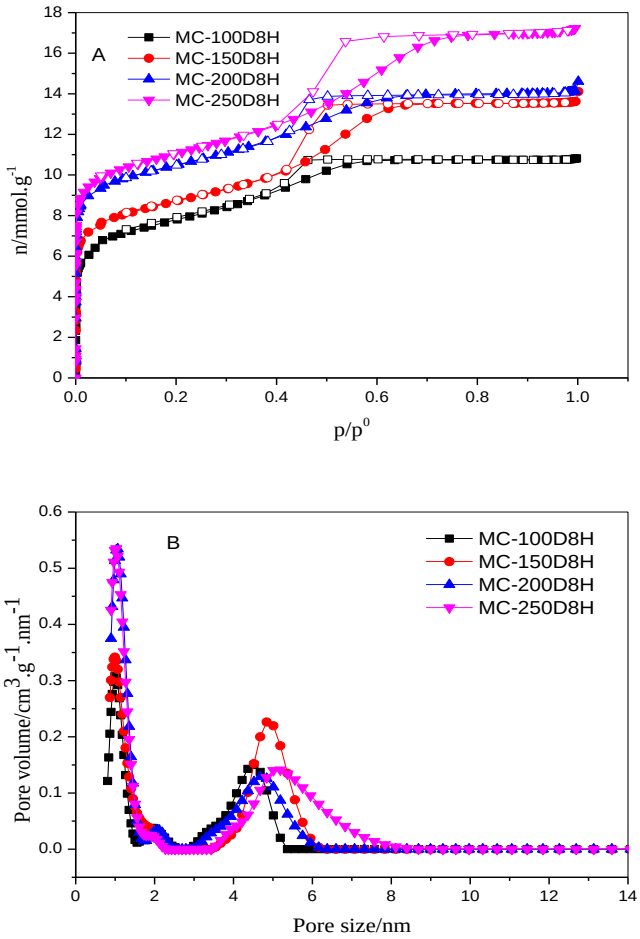

Fig. 3 N_2 sorption isotherms (A) and corresponding pore size distributions (B) of the carbon materials prepared at different temperatures for 8 h.

Tab.1 Textural properties of the mesoporous carbons and the N-doped mesoporous carbons

Sample	S_{BET}/$m^2.g^{-1}$	S_{mic}/$m^2.g^{-1}$	V/$cm^3.g^{-1}$	V_{mic}/$cm^3.g^{-1}$	CO_2 uptake/$mmol.g^{-1}$
MC-100D8H	572	342	0.37	0.14	2.08
MC-150D8H	631	394	0.47	0.17	2.30
MC-200D8H	748	509	0.49	0.23	2.73
MC-250D8H	736	493	0.60	0.22	2.69
MC-250D4H	554	320	0.46	0.13	1.85
MC-250D12H	556	310	0.52	0.12	1.79
NMC-250D8H	385	260	0.38	0.12	2.43

In order to investigate the morphology of the carbons, SEM and TEM were performed on the samples MC-100D8H and MC-250D8H. Low magnifications images (not provided here) show that both samples are composed of irregular particles, but domains of obvious regular surface intervals indicating the presence of an ordered mesostructure for MC-100D8H (Fig.4a), which can be further confirmed by its TEM image where typical stripe-like and uniformly arranged arrays are displayed through the carbon matrix (Fig.4c). This result is in line with the previous discussion on N_2 sorption and small angle XRD. At a higher curing temperature such as 250 ^oC, the ordered mesoporous structure observed on the sample MC-100D8H disappeared (sample MC-250D8H, Fig.4b), but it still exhibited well-developed mesostructures (Fig.4d). It should be pointed out that high curing temperature will give rise to great changes in the mesostructure of the carbon sample. For example, as shown in Fig.4d, the structure of the sample MC-250D8H cured at 250 ^oC exhibits worm-like mesostructure, much different from the stripe-like of MC-100D8H cured at 100 ^oC. This structural change from stripe-like to worm-like may be due to the incomplete and imperfect self-assembly between surfactant and carbon precursors at a high curing temperature. This is actually expectable since a high temperature weakens the formed H-bonding between the EO blocks of surfactant and phenolic resin, which has been considered as a driving force for the formation of ordered mesostructures.[35-37]

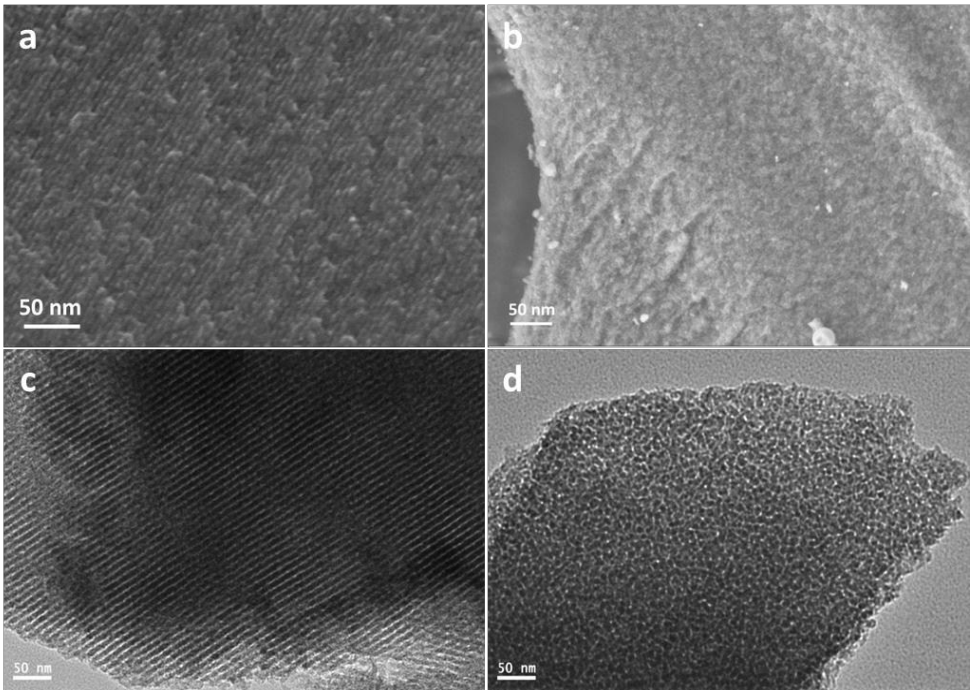

Fig.4 SEM (a,b) and TEM (c,d) images of MC-100D8H (a,c) and MC-250D8H (b,d)

Since the sample obtained at 250 ^{o}C exhibits comparatively excellent pore volume and surface area, based on such temperature, the effect of curing duration (4, 8, and 12 h) on the textural properties of the obtained carbons was further performed. Fig.5 shows the small angle XRD patterns of the obtained carbons prepared at 250 ^{o}C for different durations, similar XRD patterns were obtained for these samples, which indicates the structures of these samples are basically unaffected by the duration of thermal treatment process. However, the duration has a significant effect on the porosity of samples, indicated by the N_2 sorption isotherms in Fig.6A where large difference in N_2 sorption capacities was observed. The textural properties of these samples are shown in Tab.1. The surface area of the obtained carbons increases and then decreases as the thermal treatment time prolongs, and the sample MC-250D8H treated for 8 H exhibits the highest surface area and pore volume. This can be related to the trade-off between the self-assembly and the crosslinking of the polymeric frameworks, i.e. self-assembly was enhanced with the increasing of thermal treatment duration that benefits to the development of porous structures, while the crosslinking of polymeric frameworks makes the escape of gaseous molecules in the polymeric frameworks difficult which hinders the formation of micropores and thus lowers the micropore area. Such deduction could be confirmed by the fact that with the increasing of the thermal treatment duration, the micropore area of MC-250D12H (310 m^2/g) is significantly decreased when compared with that of MC-250D8H (490 m^2/g). In addition, the pore size also follows a similar increasing trend with the duration as the thermal temperature increased, for example, the mesopore size of MC-250D12H is increased to 5.58 nm when the thermal treatment time was from 4 H to 12 H (Fig.6B).

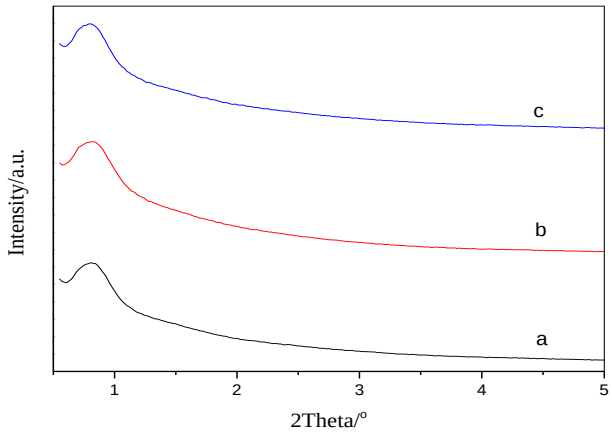

Fig.5 Small angle XRD patterns of the obtained carbons prepared at 250 °C for different time. (a) MC-250D4H, (b) MC-250D8H, (c) MC-250D12H

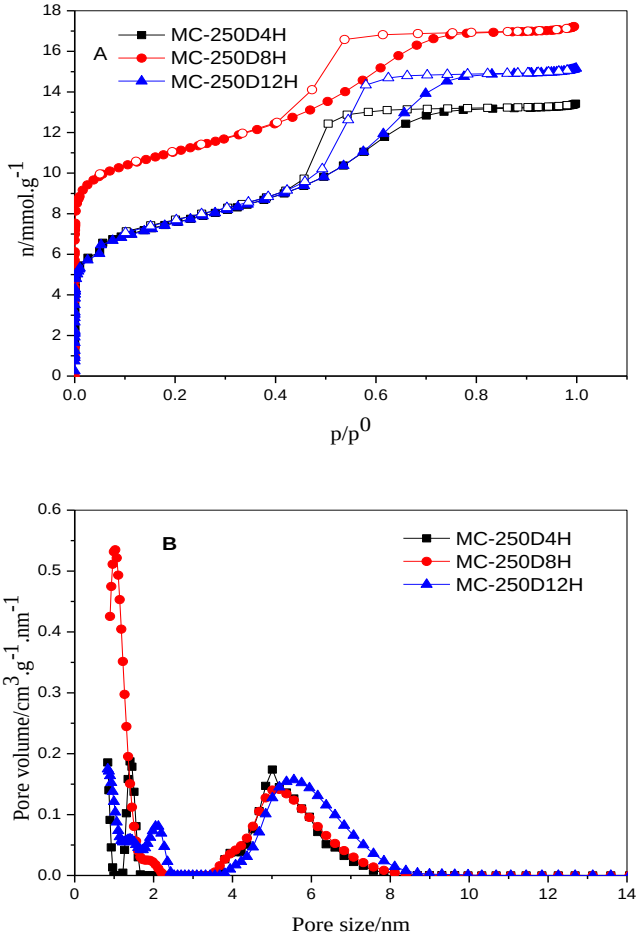

Fig. 6 N_2 sorption isotherms (A) and corresponding pore size distributions (B) of the carbon materials prepared at 250 °C for different time.

Based on the above results, it is clear that mesoporous carbon materials can be obtained by the developed one-pot melting-assisted method even without added solvents, more importantly, the porous structure can be adjusted by varying the curing temperature. This demonstrates that

the surfactant and polymer molecules possessed enough mobility in the hot and self-pressurized condition to ensure the self-assembly of surfactant-polymer composites can be properly achieved. Generally, the current strategy for the synthesis of MCs is significantly different from the most reported methods where a sacrificial hard template and/or a solvent is necessary, owing to this as well as the simplicity of the preparation itself, the method reported here is fairly promising for the scaling up of the MCs preparation and potential application.

3.2 Structural characteristics of the NMC

It has been well reported that the incorporation of electron-donating elements in the carbon matrix, such as N, can improve the adsorption selectivity for CO_2 due to the enhanced interactions between CO_2 and carbon surface. Thus, a primary study on preparation of N-doped carbon material using this one-pot melting-assisted solvent-free method was carried by simply introducing melamine as a nitrogen source in the thermal treatment process.

Fig.7 shows the N_2 sorption isotherm and corresponding PSD of the obtained N-doped carbon material (NMC-250D8H). As shown in Fig.7A, the N_2 isotherm is also of type IV with a pronounced hysteresis loop, indicating the presence of mesopores in the N-doped carbon sample. As compared with those of N-free carbons (such as MC-250D8H), although the mesostructure of NMC-250D8H is disordered, which was evidenced from the fact that there are no diffraction peaks in the small angle XRD pattern of NMC-250D8H (Fig.S1, **ESI**†), the NMC-250D8H sample still exhibits similar PSD to that of MC-250D8H (Fig.7B) and well-developed surface area and pore volume of 385 m^2/g and 0.38 cm^3/g, respectively. It should be pointed out that the disordered structure, broad pore size distribution, and decreased surface area and pore volume of NMC-250D8H as compared with pure carbon materials are probably caused by the introduction of large amounts of nitrogen source which hinders the self-assembly process of carbon precursors and template.

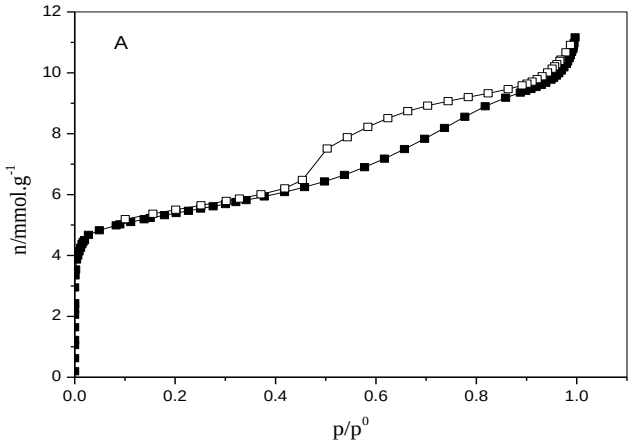

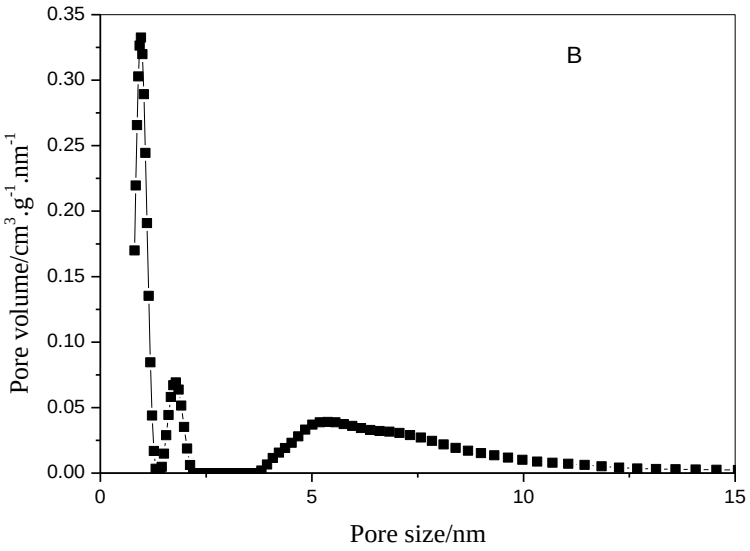

Fig. 7 N_2 sorption isotherms (A) and corresponding pore size distributions (B) of the N-doped carbon prepared at 250 ^{o}C for 8 h.

The elemental analysis reveals that the NMC-250D8H sample is composed of C, H, N, and O elements, and the nitrogen content is as high as 11.67 wt.%, this clearly indicated the effective doping of nitrogen into the carbon frameworks with this one-pot solvent-free method. To investigate the surface chemistry of the NMC-250D8H sample, XPS analysis was further performed. The XPS survey spectrum (Fig.8A) of the NMC-250D8H sample exhibits three typical peaks for C 1s, N 1s and O 1s, and the corresponding content of each element is displayed in the insert of Fig.8A. The surface nitrogen content determined from XPS measurement is 11.8 %, which is comparable to the elemental analysis, indicating the incorporated N is highly dispersed in the carbon matrix, which can be further confirmed by the subsequent elemental mapping (Fig.9) where the distribution of C, N and O elements are homogeneous. The fitting of the spectrum of N 1s (Fig.8B) reveals three nitrogen species of pyridinic nitrogen (398.1 eV), pyrrolic nitrogen (400.6 eV) and oxidized nitrogen (402.8 eV).[28,38,39]

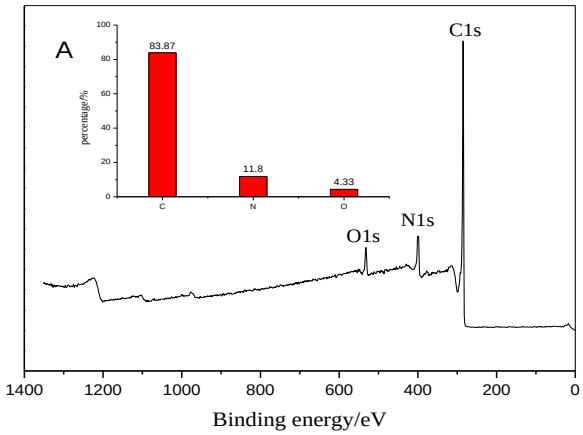

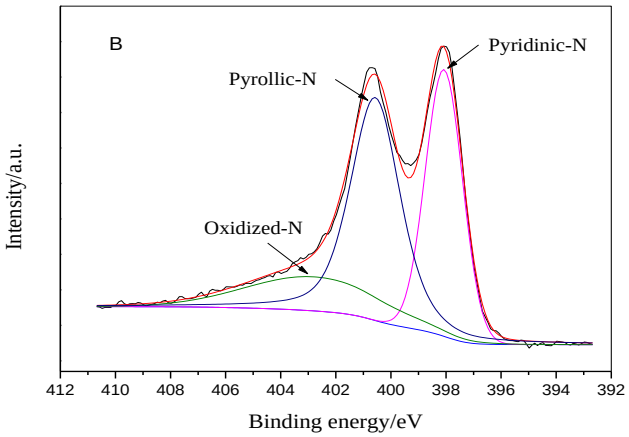

Fig.8 XPS data for the obtained NMC-250D8H sample: (A) survey; (B) N 1s

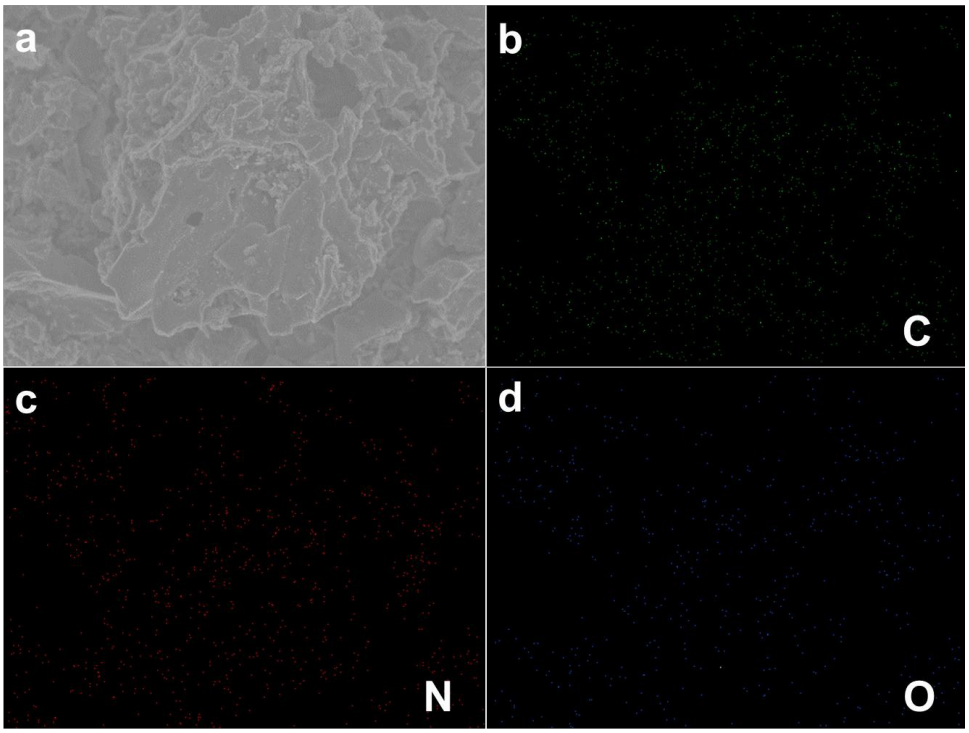

Fig.9 SEM image (a) and the corresponding C (b), N (c), O (d) elemental maps of the NMC-250D8H.

From the above results, one can see that the reported one-pot method can also be successfully used to facilely prepare N-doped mesoporous carbon materials with well-developed porosity, high nitrogen content, and highly dispersed nitrogen functionalities, which should be advantageous for gas adsorption. Bearing this in mind, CO_2 was employed as a probe molecule to test the adsorptive performance of the NMC and MCs prepared in our study.

3.3 CO_2 capture capacity

The CO_2 adsorption isotherms at 298 K are shown in Fig.10, and adsorption capacities at 1 bar are listed in Tab.1. It can be seen that the sample MC-100D8H has a CO_2 adsorption capacity of 2.08 mmol/g at 1.0 bar. With the increased curing temperature, the obtained carbon material

exhibits an improved CO_2 adsorption capacity, however, further increase in curing temperature has little effect on CO_2 adsorption capacity, with MC-250D8H being similar to MC-200D8H. The highest CO_2 adsorption capacity of ca. 2.73 mmol/g is achieved on the sample MC-200D8H. This value is comparable or higher than other similar carbons and even some of the reported nitrogen-doped carbons. For example, the activated carbon and the widely studied mesoporous carbon CMK-3 displayed 1.68 mmol/g and 2.50 mmol/g of CO_2 uptakes at 298K and 1 bar, respectively.[40,41] The nitrogen-doped mesoporous carbon shows a CO_2 uptake of 2.26 mmol/g at 298 K and 1 bar,[28] and the hollow carbon spheres with a high nitrogen loading content of 14.8 % exhibit a CO_2 capacity of 2.67 mmol/g.[32] Therefore, from the comparisons, it is clear that the obtained carbon material from this simple and inexpensive one-pot method achieves an excellent adsorption capacity for CO_2 capture. This promising CO_2 capture performances of MCs in our case can be attributed to the high surface area and highly developed hierarchical porous structures, especially large amounts of micropores, which could be confirmed by the linear relationship of the measured CO_2 adsorption capacities with surface areas and micropore areas (Fig.11).

Besides, one can see from Fig.10 that although the incorporation of N in the carbon matrix results in its surface area decreasing to 385 m^2/g (Tab.1), the lowest value among all the obtained samples in the current study, it provides a CO_2 capacity of 2.43 mmol/g. This value is much higher than some samples with higher surface area (such as MC-100D8H, MC-150D8H, MC-250D4H, and MC-250D12H), which indicates the CO_2 capture performance of the N-doped sample NMC-250D8H is clearly improved. Remarkably, this improvement on CO_2 capacity is more obvious at low pressures (Fig.10) and high temperatures (Fig.12), for example, the N-doped sample NMC-250D8H exhibits CO_2 capacities of 1.16 mmol/g (298 K and 0.15 bar) and 1.66 mmol/g (348 K and 1 bar), while the sample MC-250D8H only shows 0.91 mmol/g and 1.01 mmol/g at the same conditions. This can be attributed to the increased surface polarity and surface basic sites of NMC-250D8H due to the incorporation of basic N-containing groups in the carbon framework which have a stronger interaction with the acidic CO_2, thus leading to a higher CO_2 adsorption entropy on NMC-250D8H than that of MC-250D8H (Fig.13). Moreover, it is worth emphasizing that although the CO_2 adsorption capacity of NMC-250D8H decreases to 1.66 mmol/g with the adsorption temperature increases to 348 K (Fig.12), such capacity is among the highest value reported for N-doped carbons at the same conditions to the best of our knowledge[42-45].

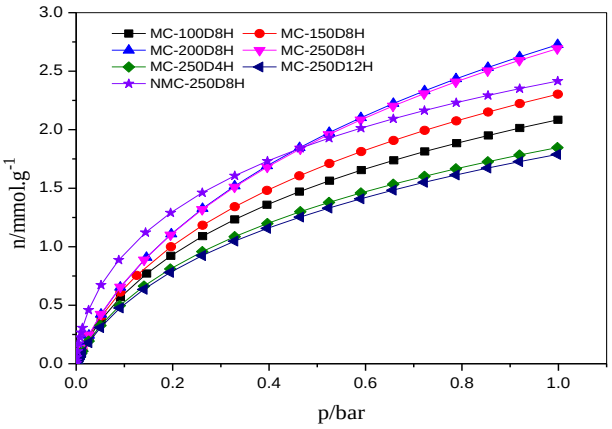

Fig.10 CO_2 adsorption isotherms at 298 K of the obtained NMC-250D8H and MCs samples

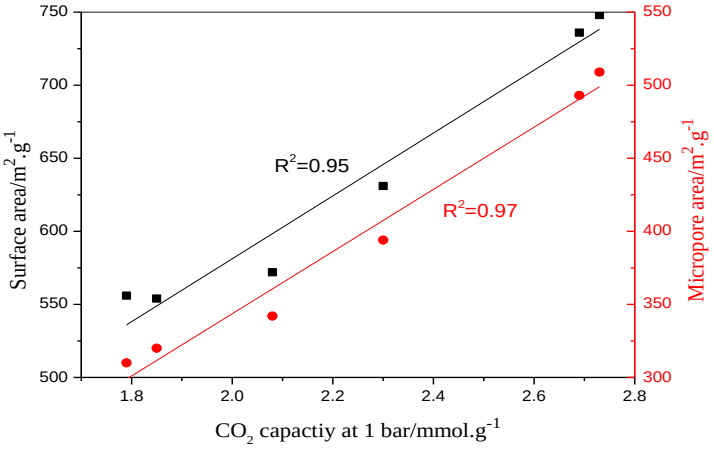

Fig.11 The linear relationship of CO_2 adsorption capacities (298 K, 1 bar) with surface area and micropore area.

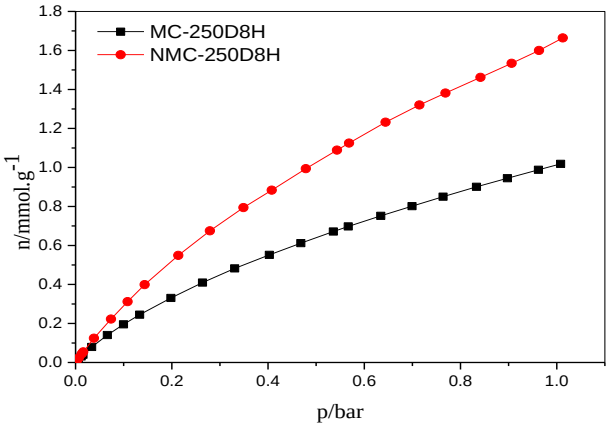

Fig.12 CO_2 adsorption isotherms at 348 K of the obtained NMC-250D8H and MC-250D8H

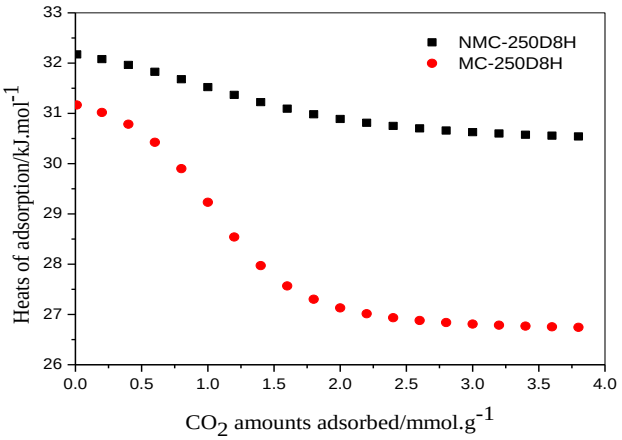

Fig.13 CO_2 adsorption heat on MC-250D8H and NMC-250D8H at different CO_2 loadings

For practical application, proper adsorbents must possess a high selectivity against other gases in addition to high CO_2 uptake. To evaluate the CO_2 separation performance of the selected

samples MC-250D8H and its N-doped counterpart NMC-250D8H, their CO_2 and N_2 isotherms at 298 K are shown in Fig.14A. The adsorption capacity of N_2 is far lower than that of CO_2 under similar conditions for both MC-250D8H and NMC-250D8H, particularly, the N_2 capacity of NMC-250D8H is less than MC-250D8H due to its low surface area. Therefore, the lower N_2 capacity and the above mentioned higher CO_2 capacity of NMC-250D8H than MC-250D8H indicate the separation performance of NMC-250D8H for CO_2 from N_2 is superior to that of MC-250D8H. Based on the ideal adsorption solution theory (IAST),[46] the CO_2/N_2 selectivity under different CO_2 concentrations in $CO2/N_2$ mixture was calculated (Section III, **ESI**†), and the results are shown in Fig.14B. It is clear that the CO_2/N_2 selectivity of NMC-250D8H is higher than that of MC-250D8H due to the stronger chemical interaction of CO_2 by the incorporated basic N species in NMC-250D8H, indicating NMC-250D8H has much better CO_2 separation capability than MC-250D8H. For example, the selectivity of NMC-250D8H is 240.7 under simulated flue gas conditions (15%CO_2, 85%N_2), while MC-250D8H exhibited an adsorption selectivity of only 21.6 at the same condition, one eleventh of the selectivity of NMC-250D8H. This value is far higher than those preciously reported for N-doped carbons (CO_2 selectivity=29-124).[31,32,45] Moreover, with the increase of CO_2 concentration in N_2, the CO_2/N_2 selectivity of NMC-250D8H dramatically increases, thus led to the selectivity difference between NMC-250D8H and MC-250D8H becoming larger. Therefore, the above results provides the fact that the N-doped sample NMC-250D8H obtained with the as-reported one-pot melting-assisted solvent-free method can be a promising candidate for CO_2 capture.

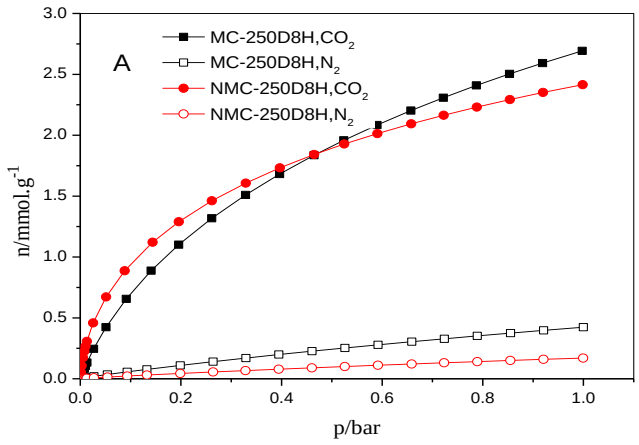

Fig.14 CO_2 and N_2 isotherms at 298 K (A) and selectivity for CO_2/N_2 (B) of the MC-250D8H and NMC-250D8H samples

3.4 Reliability of the one-pot melting-assisted solvent-free method

In order to investigate the reliability and scaling up of the one-pot synthesis method, sample MC-100D8H was selected and prepared in 3 and 10 fold scales, and the finally obtained carbon samples were denoted as MC_{x3}-100D8H and MC_{x10}-100D8H.

Fig.15 displays the CO_2 adsorption isotherms of MC_{x3}-100D8H and MC_{x10}-100D8H, as well as MC-100D8H. It shows that the CO_2 adsorption capacity of MC_{x3}-100D8H and MC_{x10}-100D8H is basically the same compared with that of MC-100D8H. This suggests that the current one-pot green method is a highly reproducible approach and can be readily scaled up with limited change in sample quality. Therefore, we believe that such a simple and effective method would significantly pave the way for practical applications of MCs and NMC materials.

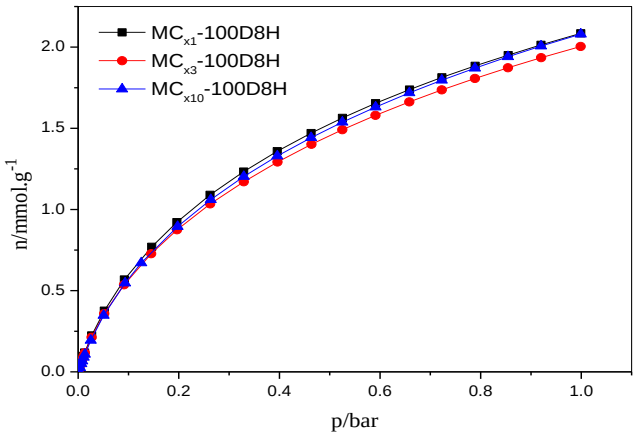

Fig.15 CO_2 isotherms at 298 K of the MC-100D8H sample prepared under 1, 3 and 10 times of raw materials

4 Conclusions

In this report, a very simple and highly effective one-pot green method was successfully developed for the facile synthesis of mesoporous carbons (MCs) and highly dispersed nitrogen incorporated mesoporous carbons (NMCs) from solid raw materials. Compared with the widely used hard template method and evaporation induced self-assembly (EISA) method, this method avoids the use of solvents and only involves a simple curing process, thus making it very convenient and fast for the large scale production of MCs and NMCs in industry.

Besides, the resultant carbon materials from this method show high surface areas, uniform pore size distributions and well-developed hierarchical porous structures. Due to these featured porous characters, the obtained carbons exhibit a considerable performance for CO_2 capture with a capacity of 2.73 mmol/g at 298 K and 1.0 bar, and a high selectivity of 21.6 for CO_2 over N_2 in simulated flue gas conditions. More importantly, the as-synthesized N-doped carbon material from this method has a high nitrogen content of 11.67 %. Due to the successful incorporation of N in the carbon matrix, the obtained N-doped carbon exhibits a significantly enhanced CO_2 capacity of 1.66 mmol/g at 348 K and an extremely high CO_2/N_2 selectivity of 240.7. Thus, we believe that this simple and effective synthesis method offers great potential for large scale production of mesoporous carbons and N-doped carbons that hold very great promise for CO_2

capture and separation in practical applications.

Notes and references

1 W. Shao, L. Z. Zhang, L. Z. Li and R. L. Lee, *Adsorpt. J. Int. Adsorpt. Soc.,* 2009, **15**, 497-505.
2 S. Choi, J. H. Drese and C. W. Jones, *ChemSusChem*, 2009, **2**, 796-854.
3 Q. Wang, J. Z. Luo, Z. Y. Zhong and A. Borgna, *Energy Environ. Sci.,* 2011, **4**, 42-55.
4 M. Bhagiyalakshmi, J. Y. Lee and H. T. Jang, *Int. J. Greenhouse Gas Control*, 2010, **4**, 51-56.
5 J. Liu, P. K. Thallapally, B. P. Mcgrail, D. R. Brown and J. Liu, *Chem. Soc. Rev.*, 2012, **41**, 2308-2322.
6 K. Wang, X. Guo, P. F. Zhao, F. Z. Wang and C. G. Zheng, *J. Hazard. Mater.*, 2011, **189**, 301-307.
7 B. B. Sakadjian, M. V. Iyer, H. Gupta and L. S. Fan, *Ind. Eng. Chem. Res.*, 2007, **46**, 35-42.
8 Z. X. Wu and D. Y. Zhao, *Chem. Commun.*, 2011, **47**, 3332-3338.
9 C. D. Liang, Z. Li and S. Dai, *Angew.Chem. Int. Ed.*, 2008, **47**, 3969-3972.
10 Y. D. Xia, R. Mokaya, G. S. Walker and Y. Q. Zhu, *Adv. Energy Mater.,* 2011, **1**, 678-683.
11 B. R. Ryoo, S. H. Joo, M. Kruk and M. Jaroniec, *Adv. Mater.*, 2001, **13**, 677-681.
12 T. Kyotani, T. Nagai, S. Inoue and A. Tomita, *Chem. Mater.*, 1997, **9**, 609-615.
13 B. Sakintuna and Y. Yurum, *Micro. Meso.Mater.*, 2006, **93**, 304-312.
14 S. Jun, S. H. Joo, R. Ryoo, M. Kruk, M. Jaroniec, Z. Liu, T. Ohsuna and O. Terasaki, *J. Am. Chem. Soc.*, 2000, **122**, 10712-10713.
15 M. Kruk, M. Jaroniec, R. Ryoo and S. H. Joo, *J. Phys. Chem. B*, 2000, **104**, 7960-7968.
16 K. Hou, A. F. Zhang, L. Gu, M. Liu and X. W. Guo, *J. Colloid Interf. Sci.*, 2012, **377**, 18-26.
17 B. R. Ryoo, S. H. Joo and S. Jun, *J. Phys. Chem. B*, 1999, **103**, 7743-7746.
18 J. Lee, S. Yoon, T. Hyeon, S. M. Oh and K. B. Kim, *Chem. Commun.*, 1999, **21**, 2177-2178.
19 J. S. Beck, J. C. Vartuli, W. J. Roth, M. E. Leonowicz, C. T. Kresge, K. D. Schmitt, C. T. W. Chu, D. H. Olson, E. W. Sheppard, S. B. McCullen, J. B. Higgins and J. L. Schlenker, *J. Am. Chem. Soc.*, 1992, **114**, 10834-10843.
20 C. D. Liang, K. L. Hong, G. A. Guiochon, J. W. Mays and S. Dai, *Angew.Chem., Int. Ed.*, 2004, **43**, 5785-5789.
21 F. Q. Zhang, Y. Meng, D. Gu, Y. Yan, C. Yu, B. Tu and D. Y. Zhao, *J. Am. Chem. Soc.*, 2005, **127**, 13508-13509.
22 Y. Wan, X. F. Qian, N. Q. Jia, Z. Y. Wang, H. X. Li and D. Y. Zhao, *Chem. Mater.*, 2008, **20**, 1012-1018.
23 J. P. Yang, Y. P. Zhai, Y. H. Deng, D. Gu, Q. Li, Q. L. Wu, Y. Huang, B. Tu and D. Y. Zhao, *J. Colloid Interf.Sci.*, 2010, **342**, 579-585.
24 M. Bhagiyalakshmi, P. Hemalatha, M. Ganesh, P. M. Mei and H. T. Jang, *Fuel*, 2011, **90**, 1662-1667.
25 C. Booth and D. Attwood, *Macromol. Rapid Commun.*, 2000, **21**, 501-527.
26 C. Yu, B. Tian, J. Fan, G. D. Stucky and D. Zhao, *Chem. Commun.*, 2001,**24**, 2726-2627.
27 S. A. Wohlgemuth, R. J. White, M. G. Willinger, M. M. Titiricia and M. Antonietti, *Green Chem.*, 2012, **14**, 1515-1523.
28 Z. Z. Zhang, C. M. Zhu, N. N. Sun, H. Wang, Z. Y. Tang, W. Wei and Y. H. Sun, *J. Phys. Chem. C*, 2015, **119**, 9302-9310.
29 W. F. Chen, L. F. Yan and P. R. Bangal, *Carbon*, 2010, **48**, 1146-1152.
30 P. X. Han, Y. H. Yue, L. X. Zhang, H. X. Xu, Z. H. Liu, K. J. Zhang, C. J. Zhang, S. M. Dong, W. Ma and G. L. Cui, *Carbon*, 2012, **50**, 1355-1362.
31 X. Y. Ma, M. H. Cao and C. W. Hu, *J. Mater. Chem. A*, 2013, **1**, 913-918.
32 S. S. Feng, W. Li, Q. Shi, Y. H. Li, J. C. Chen, Y. Ling, A. M. Asiri and D. Y. Zhao, *Chem. Commun.*, 2014, **50**, 329-331.
33 P. Alexandridis, T. A. Hatton, *Colloids Surf. A*, 1995, **96**, 1-46.
34 C. Boissiere, A. Larbot, A. Van der Lee, P. J. Kooyman, E. Prouzet, *Chem. Mater.,* 2000, **12**, 2902-2913.
35 C. D. Liang and S. Dai, *J. Am. Chem. Soc.*, 2006, **128**, 5316-5317.

36 S. Tanaka, Y. Katayama, M. P. Tate, H. W. Hillhouse and Y. Miyake, *J. Mater. Chem.*, 2007, **17**, 3639-3645.
37 Q. Y. Hu, R. Kou, J. B. Pang, T. L. Ward, M. Cai, Z. Z. Yang, Y. F. Lu and J. Tang, *Chem. Commun.*, 2007,**6**, 601-603.
38 J. Y. Yu, M. Y. Guo, F. Muhammad, A. F. Wang, F. Zhang, Q. Li and G. S. Zhu, *Carbon*, 2014, **69**, 502-514.
39 Z. X. Wu, P. A. Webley and D. Y. Zhao, *J. Mater. Chem.*, 2012, **22**, 11379-11389.
40 M. S. Park, S. E. Lee, M. I. Kim and Y. S. Lee, *Carbon Letters*, 2015, **1**, 45-50.
41 Z. Z. Zhang, H. Wang, X. Q. Chen, C. M. Zhu, W. Wei and Y. H. Sun, *Adsorption*, 2015, **21**, 77-86.
42 Q. Li, J. P. Yang, D. Feng, Z. X. Wu, Q. L. Wu, S. S. Park, C. S. Ha and D. Y. Zhao, *Nano. Res.*, 2010,**3**, 632-642.
43 C. Pevida, T. C. Drage and C. E. Snape, *Carbon*, 2008, **46**, 1464-1474.
44 G. P. Hao, W. C. Li, D. Qian and A. H. Lu, *Adv. Mater.*, 2010, **22**, 853-857.
45 R. Li, X. Q. Ren, X. Feng, X. G. Li, C. W. Hu and B. Wang, *Chem. Commun.*, 2014, **50**, 6894-6897.
46 A. L. Myers and J. M. Prausnitz, *AIChE J.*,1965, **11**, 121-127.

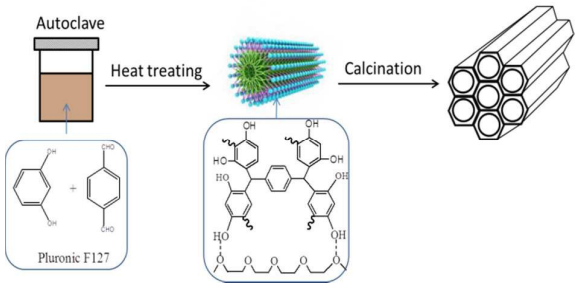

A facile one-pot melting-assisted solvent-free method to synthesize mesoporous carbon and N-doped carbon with excellent CO_2 capture properties.